

**A Molecular Dynamics Study of the Effect of Asphaltenes on Toluene/Water Interfacial
Tension: Surfactant or Solute?**

Cuiying Jian,^{†,‡} Qingxia Liu,[‡] Hongbo Zeng,^{*,‡} and Tian Tang^{*,†}

[†]Department of Mechanical Engineering,

and [‡]Department of Chemical and Materials Engineering,

University of Alberta, Edmonton,

AB, T6G 1H9, Canada

* Corresponding author:

Phone: +1-780-492-1044. Fax: +1-780-492-2881. E-mail: hongbo.zeng@ualberta.ca (H.Z.).

Phone: +1-780-492-5467. Fax: +1-780-492-2378. E-mail: tian.tang@ualberta.ca (T.T.).

ABSTRACT:

A series of molecular dynamics simulations were performed to investigate the effects of model asphaltene on the toluene/water interfacial tension (IFT) under high temperature and pressure conditions. In the absence of model asphaltene, the toluene/water IFT monotonically decreases with increasing temperature; while with the presence of model asphaltene, especially at high concentrations, such monotonic dependence no longer holds. Furthermore, in contrast with the decreasing trend of IFT with increasing model asphaltene concentration at low temperature (300 K), increasing concentration at high temperature (473 K) leads to increasing IFT. This relation can even be non-monotonic at moderate temperatures (373 K and 423 K). Through detailed analysis on the distribution of model asphaltene with respect to the interface, such complex behaviors are found to result from the delicate balance between miscibility of toluene/water phases, solubility of model asphaltene, and hydrogen bonds formed between water and model asphaltene. By increasing temperature, the solubility of model asphaltene in toluene is enhanced, leading to their transition from being a surfactant to being a solute. The effect of pressure was found to be very limited under all model asphaltene concentrations. Our results here present, for the first time, a complete picture of the coupled effect of (high) temperature and asphaltene concentration on IFT, and the methodology employed can be extended to many other two-phase or multiphase systems in the presence of interface-active chemicals.

KEYWORDS:

Interfacial tension, high temperature, surfactant, solute, asphaltene

1. INTRODUCTION

Interfacial tension (IFT) is a quantity of great importance in multiphase processes such as oil production. IFT is related to the stability of emulsions, interfacial adsorption of surface-active components, critical micelle concentration of heavy oil compounds, etc.¹⁻⁴ Fundamental knowledge on IFT not only helps us with understanding the dynamics and morphologies of multiphase systems in oil production,⁵⁻⁸ but also sheds lights on how to destabilize undesired emulsions as well as remove problematic compounds.¹⁻⁴ Because of this, significant amount of experimental work has been dedicated to investigating oil/water IFT under different conditions: solvents, salinity, presence of surface-active compounds, temperature (T), and pressure (P),⁹⁻¹¹ to name a few. In parallel with experiments, to fully understand the underlying mechanisms responsible for IFT variations, there is also a great need of computational studies that can provide atomistic evidences for experimental observations.

Over the past decade, computational tools, such as molecular dynamics (MD) simulation, have been widely employed to investigate the bulk aggregation and interfacial adsorption of heavy oil compounds, i.e. asphaltenes.¹²⁻¹⁵ These works have greatly helped to explain experimental observations, as well as to resolve existing discrepancies. For instance, using model compounds, MD studies have clarified the effect of core size, heteroatoms, and side-chain length on the aggregation behaviors of asphaltenes.¹²⁻¹⁵ On the other hand, little computational work has been done to investigate oil/water IFT, in particular, with the presence of surface-active components such as asphaltenes. Mikami and co-workers¹⁶ performed the pioneering work in this direction, and it was observed that increasing asphaltene concentration decreased oil/water IFT, consistent with experimental observations.¹⁷⁻¹⁹ However, the bulk concentrations, at which IFT reduction was observed in simulations and experiments, differed by two orders of

magnitude.^{3,16,20} To probe the cause of this discrepancy, recently a novel approach, combining the strength of MD simulations and pendant drop IFT measurements, was proposed²¹ for investigating the IFT between organic solvent and water in the absence and presence of model asphaltenes. It was revealed that²¹ the reduction of oil/water IFT was determined by the surface concentration, rather than bulk concentration, of the interfacially active components. To achieve a surface concentration similar to that in experiments, much higher bulk concentrations must be adopted in simulations, given the large surface-to-volume ratio at nano scale.

Based on these results, the effect of T on IFTs was further investigated.²² It was found that elevating T (from 300 K to 350 K) decreased the IFT by increasing the miscibility of toluene and water phases. The calculated trends are consistent with the effects of T reported in literature.²³⁻²⁶ With the presence of asphaltenes, the effect of temperature was alleviated. That is, in comparison with their counterparts without asphaltenes, the decrement in IFT caused by increasing T was less evident with the presence of asphaltenes. This interesting coupling is caused by the extent of asphaltene accumulation on the interface, which can be modified by the change of T. While this work provided atomic-level explanations on the effect of T, the range of T studied is much narrower than that encountered during industrial processing.²⁷ Therefore, it is of great importance to extend the T range. Furthermore, from the computational aspect, most available protocols and force fields are developed for simulations near room T and P. It is thus of general interest to investigate their applicability at high T and P. This benchmarking is useful for many other studies where interfaces are present under drastically varied external conditions.

The remainder of this article is organized as follows: the systems studied along with simulation method are introduced in section 2; results are discussed in section 3, and final conclusions are presented in section 4.

2. SIMULATION METHODS

In this work, toluene was selected as a model oil phase, considering its wide usage in separating asphaltenes from fine solids and bitumen. Violanthrone-79 (VO-79, $C_{50}H_{48}O_4$) was adopted as the model asphaltene compound, for which the chemical structure is shown in Figure 1. The rationale for choosing VO-79 has been elaborated in our previous work.^{21,28} Briefly, the molecular structure of VO-79 is similar to that of the island-type asphaltenes,²⁹ and its oxygen content (9.0%) is relatively close to that of the asphaltene fractions stabilizing water/oil emulsions (4.42%–5.54%).^{30,31}

2.1. Systems Simulated. In total, 16 systems were constructed to investigate the IFT of toluene/water interface at high T and high P, and their details are summarized in Table 1.

The first 4 systems in Table 1 were built in the absence of VO-79, each simulated at a specified T and P: system T373-P100 at 373 K and 100 bar, T423-P100 at 423 K and 100 bar, T473-P100 at 473 K and 100 bar, and T473-P200 at 473 K and 200 bar. As experimental IFT values under these conditions (except 473 K and 100 bar) are available in literature,⁹ these systems were used to validate our theoretical protocols. The additional simulation at 473 K and 100 bar can allow us to probe the effect of P separately from the effect of T (see discussions in section 3).

The other systems, each containing a certain amount of VO-79, were then built to probe the role of VO-79 in modulating the effect of T and P. Under each T/P condition, 3 different concentrations of VO-79 were studied, corresponding to 180, 540, and 720 molecules respectively. While these numbers represent enormous bulk concentrations given the small sizes of our simulation boxes, they are necessary in order for the surface concentration of VO-79 to

reach the critical threshold in experiments (performed at 300 K) below which no apparent change of the toluene/water IFT was caused by VO-79.²¹ It is also noted that the pressure employed in our simulations are quite high (100 bar or 200 bar); such high values are necessary to maintain the liquid state for water and toluene.

The initial configurations were constructed using the procedure reported in our previous work.²¹ Briefly, for the first four systems in Table 1, a box of dimension 6*6*3 nm³ was first filled with water molecules. Then the water box was expanded in the *z* direction for 3 nm to reach a final dimension of 6*6*6 nm³. Following this, the rest of the box was filled with toluene molecules, generating the water/toluene interface in the *xy* plane. When constructing the initial configurations for systems containing VO-79 molecules, a box of dimension 12*12*12 nm³ was first randomly filled with water molecules, and then the box was expanded in the *z*-direction to a length of 24 nm. After expansion, we placed, adjacent to the water phase, 180 VO-79 molecules in systems T373-P100-VO180, T423-P100-VO180, T473-P100-VO180 and T473-P200-VO180. These 180 VO-79 molecules were arranged to have their polyaromatic cores perpendicular to the interface but parallel with one another, forming a single layer on the water surface. Two additional layers of VO-79 were introduced into systems T373-P100-VO540, T423-P100-VO540, T473-P100-VO540 and T473-P200-VO540 to form a three-layer interface; similarly, in systems T373-P100-VO720, T423-P100-VO720, T473-P100-VO720 and T473-P200-VO720, three additional layers were introduced, resulting in a four-layer interface. Finally, the rest of the box was filled randomly with toluene molecules.

2.2. Simulation Details. The topologies for VO-79 and toluene molecules was built previously^{21,32} based on the GROMOS96 force field parameter set 53A6,³³ and they were

directly applied here. For the aqueous phase, a simple-point-charge model³⁴ was used for water, which has been extensively tested for interfacial studies.³⁵⁻³⁷

All simulations were performed using GROMACS (version 4.6.5).³⁸⁻⁴¹ For each system, static structure optimization was first performed to ensure the maximum force is less than 1000.0 kJ/(mol nm). Then full dynamics simulations were conducted in NP_nAT ensemble for 10 ns for the four systems without VO-79 molecules, and for 30 ns for all the other systems. Here P_n and A are, respectively, the normal pressure perpendicular to the interface (i.e. in z direction) and the interfacial area in the xy plane. During all dynamics simulations, a time step of 2 fs was adopted; a twin-range cutoff scheme was used to treat van der Waals interaction; particle-mesh Ewald⁴² method was employed to handle long-range electrostatic interaction. Furthermore, average P_n was kept constant in each system using Parrinello–Rahman barostat,⁴³ and average T was maintained using a velocity rescaling thermostat.⁴⁴ The velocity rescaling thermostat adopted here is based on correctly reproducing the distribution of kinetic energy under constant temperature and thus is an accurate method.⁴⁴

The topology constructed and simulation parameters chosen have been widely tested, against experimental measurements wherever available, in our previous work on the aggregation of model asphaltene in bulk solvents, the adsorption of asphaltene onto oil/water interface, and the interfacial structure formed by asphaltene.^{15,21,32} The applicability of NP_nAT ensemble for investigating IFT, as well as the procedure to calculate IFT, was described and validated in our previous work.^{21,22} Appropriate post processing tools in GROMACS³⁸⁻⁴¹ were used for analysis and VMD⁴⁵ for visualization.

3. RESULTS AND DISCUSSION

The IFT values of toluene/water interface in the absence of VO-79 are calculated and listed in Table 2; in comparison, experimental values available in literature⁹ are also presented. The computational results reproduced all experimental values with an absolute error < 5%. Therefore, our simulation protocols, including the employment of NP_nAT ensemble and the usage of GROMOS96 force field, are robust and can be applied when investigating IFT at high T and high P. In the following, we first present the coupled effect of T and VO-79 concentration in section 3.1, and the effect of pressure will be discussed in section 3.2.

3.1. Coupled Effect of T and VO-79 Concentration. Detailed examination of Table 2 shows that, with increasing T but constant P (100 bar), the IFT exhibits a decreasing trend. Such T dependence resembles the trend found in simulations performed at relatively low T (300 and 350 K) and low P (1 bar).^{21,22} To probe whether similar influences of T can be observed with the presence of VO-79, Figure 2 plots the IFT vs. the number of VO-79 molecules (denoted as M hereafter), each curve representing a particular T/P condition as indicated by the legend. We will first discuss the three curves corresponding to P=100 bar, leaving the discussion on the effect of P to section 3.2.

The first observation is that at low and moderate VO-79 concentrations ($M \leq 540$), increasing T leads to a reduction in IFT, consistent with the trends observed in Table 2. However, at extremely high concentration ($M = 720$), the effect of T on IFT is different. Specifically, while the IFT at 473K is still the lowest, the IFT at 423 K is almost identical to that at 373 K. Moreover, at a given T, complex dependence of IFT on the VO-79 concentration is observed. While it is a well-known result at room T that¹⁷⁻¹⁹ increasing M leads to decrease in the

IFT, such a trend is not observed in Figure 2. At 473 K, increasing M in fact causes a monotonic increase in IFT. At 423 K, the IFT first stays almost constant as M is increased from 0 to 180, then increases with M, and finally decreases after M reaches 540. That is, the variation of IFT with M is non-monotonic, and there exists a transition value (denoted as M_c , equal to 540 here) at which the trend changes from increasing to decreasing. At 373 K, a non-monotonic relation is again observed, but the transition occurs at a smaller M_c (= 180).

In previous simulations performed at 300 and 350 K,^{21,22} it was demonstrated that increasing T can enhance the miscibility of two immiscible phases (water and toluene), leading to IFT reduction. For the range of temperature studied here, in the absence of VO-79, the toluene/water IFT again follows a monotonically decreasing trend (Table 2), thus demonstrating that without VO-79, the IFT is still mainly governed by the miscibility of toluene and water phases. With the presence of VO-79, to probe the effect of T on toluene/water miscibility, we calculated the cumulative numbers of toluene atoms around the center of mass (COM) of the water phase for each concentration studied.

Firstly, Figure 3a plots the cumulative numbers for the three systems with 180 VO-79 molecules, all simulated at 100 bar but at different temperatures. The curves from top to bottom correspond to, respectively, the highest (473 K), intermediate (423K) and lowest (373K) temperatures, suggesting that at this concentration, higher T can increase the miscibility of toluene and water phases. Given the identical composition of these three systems, the different miscibility observed here suggests that lifting T could affect the distribution of each component in the bulk phases and near the interface. To investigate this, for the same three systems we plotted the density profiles of water, toluene and VO-79 along z-axis (perpendicular to the water/toluene interface) in Figure 3b. Drastic differences are found in the distribution of VO-79

molecules among the 3 systems. In T373-P100-VO180, the dotted line, representing VO-79 molecules, has a prominent peak near the intersection of dashed (water) and solid (toluene) lines, suggesting that VO-79 molecules tend to accumulate near the interface and form a protective layer, inhibiting direct contact between toluene and water. When T is increased to 423 K, the height of the peak in the dotted line is reduced, meanwhile its horizontal span is increased, indicating that VO-79 molecules are more likely to stay in the bulk toluene phase. When T is further increased to 473 K, the peak in the dashed line essentially disappears and VO-79 molecules are almost homogeneously distributed in the bulk toluene phase. The enhanced solubility of VO-79 in toluene at higher T facilitates direct “contact” between water and toluene molecules, which further helps to increase the miscibility of the two phases.

We further investigated systems containing 540 and 720 VO-79 molecules, and the density profiles for these systems are plotted in Figures 4a and 4b, respectively. In both figures, with increasing T the dotted lines (representing VO-79 molecules) gradually shift towards the right while the solid lines (representing toluene) move towards the left, suggesting increased solubility of VO-79 in toluene, their reduced accumulation at the interface and better miscibility of toluene/water phases (for the cumulative number of toluene atoms around water COM in these systems, see Figure S1 in Supporting Information).

Given the same increased toluene/water miscibility at higher T observed in Figures 3 and 4, one may expect the IFT to decrease with increasing T, similar to simulations performed at 300 K and 350 K.^{21, 22} However, as mentioned before (Figure 2), while this is true for the systems containing 180 and 540 VO-79 molecules, with 720 VO-79 molecules, increasing T does not necessarily lead to reduction in IFT (IFT values in T373-P100-VO720 and T423-P100-VO720 are almost identical). This apparent discrepancy seems to suggest that there may be other

mechanisms, associated with the existence of VO-79, which can act in ways opposite to the effect of toluene/water miscibility on IFT.

When VO-79 accumulates on the toluene/water interface, the heteroatoms (oxygen here) can form hydrogen bonds with water, and at room T the number of hydrogen bonds (N_{HB}) was found^{21,22} to correlate with the IFT: increase in N_{HB} leads to reduced IFT. For the high T systems studied here, we calculated N_{HB} and plotted them in Figure 5. Drastic differences can be found among systems with different number, M , of VO-79 molecules. When $M = 180$, N_{HB} increases as T increases, but the magnitude of increase is quite small. When $M = 540$, N_{HB} at 423 K and 473 K are similar and both are smaller than that at 373 K. For $M = 720$, N_{HB} follows a completely different order compared to the case of $M = 180$: it decreases as T increases, with a large difference among the three cases. With large M , the apparently smaller N_{HB} at higher T indicates less accumulated VO-79 near the interface and better solubility of VO-79 in bulk toluene, consistent with the density profile discussed before (Figure 4).

The results above allow us to identify, for systems with a high VO-79 concentration, two competing effects as T is increased: 1) increased miscibility of toluene/water phases, which tends to reduce IFT; and 2) decreased N_{HB} between VO-79 and water, which tends to increase IFT. For the three systems in Figure 4b (720 VO-79 molecules), while the miscibility of toluene and water is still enhanced at 423 K compared to that at 373 K (Figure S1, Supporting Information), N_{HB} is significantly decreased (Figure 5), which leads to the similar IFT values observed for systems T373-P100-VO720 and T423-P100-VO720 (Figure 2). When T is further increased from 423K to 473K, the drop in N_{HB} is less significant (Figure 5) and the enhanced miscibility (Figure S1, Supporting Information) dominates, leading to an overall reduction in the IFT (Figure 2). Contrarily, at low or moderate VO-79 concentrations ($M = 180$ or 540), the change of N_{HB} with

T is not as significant (especially when $M = 180$) as in the case of high concentration ($M = 720$). Therefore, the IFT is mainly modulated by miscibility, resulting in the monotonic decreasing trend of IFT with increasing T.

From the density profiles of VO-79 (Figures 3 and 4), it has been seen that VO-79 migrates from the interface towards bulk toluene when T is increased. This suggests two roles the VO-79 molecules can play in our systems: as a surfactant which mainly accumulates near the interface, or as a solute which are largely distributed in bulk toluene. Their transition from one role to another can help us understand another phenomenon observed in Figure 2, viz., the variation of IFT with VO-79 concentration is T-dependent. At low T (300 K studied in our previous work^{21,22}), VO-79 molecules have extremely limited solubility in toluene; as such they accumulate at the toluene/water interface and act like surfactant even at very low VO-79 concentration ($M = 32$). In this case, increasing VO-79 concentration enhances their accumulation near the interface, and causes N_{HB} to increase and water/toluene IFT to decrease (above a threshold of VO-79 concentration^{21,22}). At very high T (473 K), the solubility of VO-79 is significantly lifted, and these molecules behave like solute which can be easily dissolved in toluene even at extremely high concentration ($M = 720$). Because the VO-79 molecules prefer to stay in the bulk toluene rather than near the toluene/water interface, their surface excess is negative. According to the Gibbs adsorption isotherm,⁴⁶ the surface excess Γ (kg/m^2) is given by

$$\Gamma = \frac{-M_m}{RT} \frac{d\gamma}{d \ln c}, \quad (1)$$

where M_m is the molar mass of the solute (VO-79), c is the bulk concentration of VO-79 (mol/L), R is the universal gas constant ($\text{J}/(\text{K mol})$), and γ is the IFT (N/m). Since Γ is negative,

$\frac{dy}{d\ln c} > 0$, which implies that IFT will increase as the concentration of VO-79, as a solute, increases.

The non-monotonic relation between IFT and M at 373K and 423K (Figure 2) can also be explained based on the different roles the VO-79 molecules play. At these intermediate temperatures, across the range of M applied, VO-79 molecules do not only simply serve as a surfactant or solute. Rather, below a transition concentration ($M < M_c$), they have little accumulation on the interface and act like solute. In this concentration range, increasing M tends to increase IFT. When $M > M_c$, VO-79 molecules act like surfactant, and increasing its concentration decreases IFT. Increasing T broadens the range of concentration where VO-79 can serve as solute; hence M_c is larger at 423K. The different roles of VO-79 in all of our simulations (including some from previous work^{21,22}) are summarized in Figure 6, where filled circles represent solutes, empty ones are surfactants, and half-filled ones represent transition between the two roles. It is clear that the position of M_c , indicated by the half-filled circles, shift to the right as T is increased.

3.2. Effect of P. Compared to T, increasing P only slightly changed toluene/water IFT in the absence of VO-79 (Table 2). Such small influence of P was also reported for benzene/water interface in absence of surface active molecules, where the IFT values were found to vary only 2-3 mN/m over the range of ~100 bar to ~1400 bar.⁴⁷ With the presence of VO-79, the influence of P on IFT as seen in Figure 2 is still very small, resembling literature findings on heavy crude oil/brine interface in presence of asphaltenes over the range of ~0 bar to ~170 bar.²⁶ Consistent with this, density profiles as well as number of hydrogen bonds in systems investigated at 473 K and 200 bar are quite similar to those at 473 K and 100 bar (for comparison, see Section S2,

Supporting Information). The observations can be understood by examining equation (1), which does not have any explicit dependence on P. This explains why P has marginal effects on the IFT at high T where VO-79 are readily dissolved.

3.3 Implications. To our knowledge, this is the first set of MD simulations that systematically investigate the effect of large values of T and P on water/toluene IFT, particularly with the presence of model asphaltene (VO-79) molecules. We demonstrated the applicability of GROMOS96 force field⁴⁷ and MD simulation in NP_nAT ensemble for investigating interfacial properties at high T and high P, which can support many other studies involving interfaces, for instance, in bio systems.⁴⁸

More importantly, together with our previous study,^{21,22} the results reported here have generated a more complete picture of IFT variation with model asphaltene concentrations and external environmental conditions (see Figure 6), which can be used for modulating IFTs during industrial processing.

CONCLUSIONS

In this work, we performed a series of MD simulations to investigate the effects of high temperature and high pressure on toluene/water IFT in the absence and presence of model asphaltenes. It was revealed that compared to temperature, pressure has marginal effect on IFT, regardless of the VO-79 concentration. In the absence of VO-79, the IFT monotonically decreases with increasing temperature, as a result of the increased miscibility of water/toluene phases. In contrast, with the presence of VO-79 molecules, the relation between IFT and temperature is concentration-dependent. At low and moderate concentrations, increasing

temperature monotonically decreases IFT, similar to the case without VO-79. At high concentrations, the monotonic dependence diminishes, and the IFT values at 373 K and 423 K are almost identical. Such complex behaviors are caused by two competing factors: miscibility of toluene/water phases and hydrogen bonding between VO-79 and water molecules. At high concentrations, increasing temperature enhances toluene/water miscibility, while simultaneously reducing the number of hydrogen bonds between VO-79 and water due to the increased solubility of VO-79 in bulk toluene. Further investigation shows that such increased solubility leads to completely different relations between IFT and VO-79 concentration at different temperatures. The relation is monotonically decreasing at low temperature (300 K, 350 K), first increasing and then decreasing at moderate temperature (373 K, 423 K), and monotonically increasing at high temperature (473 K). By increasing temperature, the solubility of model asphaltene in toluene is lifted, leading to the transition of the model asphaltene from being a surfactant to being a solute. The results here generate a complete picture of toluene/water IFT under different environmental conditions, and can help with modulating IFT during industrial processing.

ACKNOWLEDGMENTS

We acknowledge the computing resources and technical support from Western Canada Research Grid (WestGrid). Financial support from the Natural Science and Engineering Research Council (NSERC) of Canada, Alberta Innovates – Energy and Environment Solutions (AI-EES) and Nexen Energy ULC is gratefully acknowledged.

ABBREVIATIONS

A: interfacial area in the xy plane

c: bulk concentration of violanthrone-79 in equation (1)

COM: center of mass

IFT: interfacial tension

M: number of violanthrone-79 molecules

M_c : transition value of M at which the interfacial tension changes from increasing with M to decreasing with M

M_m : molar mass of violanthrone-79 in equation (1)

MD: molecular dynamics

N_{HB} : number of hydrogen bonds

P: pressure

P_n : the normal pressure perpendicular to the interface (i.e. in z direction)

R: universal gas constant in equation (1)

T: temperature

VO-79: violanthrone-79

Γ : surface excess in equation (1)

γ : interfacial tension in equation (1)

SUPPORTING INFORMATION

Cumulative number of toluene atoms around water COM in systems containing 540 and 720 VO-79 molecules, comparison on the density profiles and number of hydrogen bonds between systems simulated at 473 K and 100 bar and those at 473 K and 200 bar.

REFERENCES

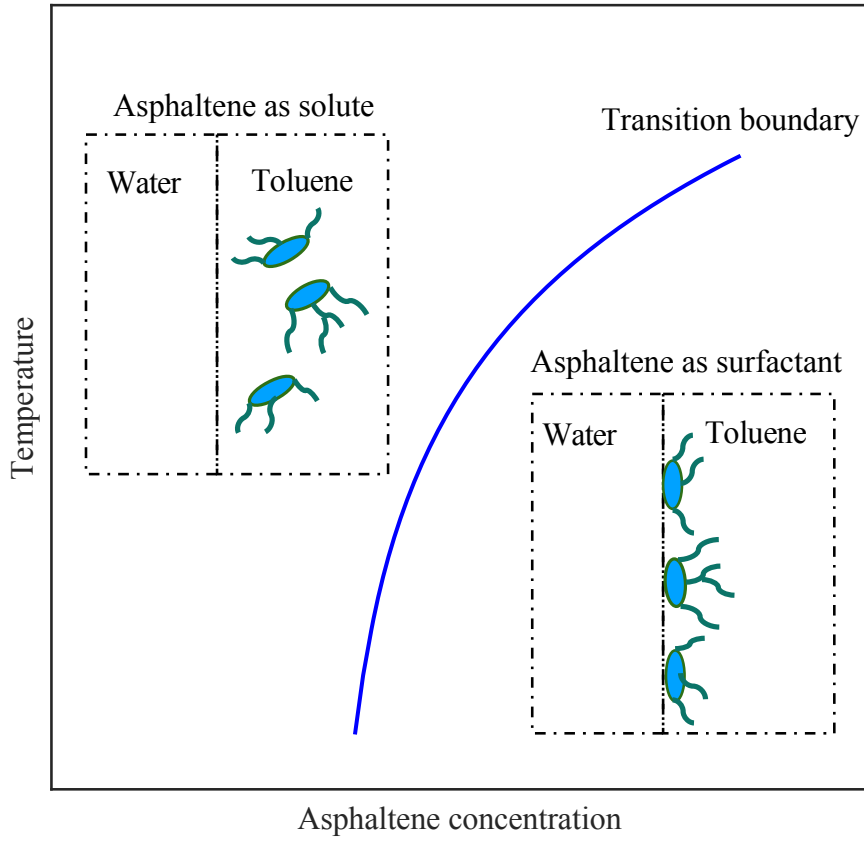
1. Poteau, S.; Argillier, J.; Langevin, D.; Pincet, F.; Perez, E. *Energy Fuels* **2005**, *19*, 1337-1341.
2. Yan, Z.; Elliott, J. A.; Masliyah, J. H. *J. Colloid Interface Sci.* **1999**, *220*, 329-337.
3. Gao, S.; Moran, K.; Xu, Z.; Masliyah, J. *J. Phys. Chem. B* **2010**, *114*, 7710-7718.
4. Rogel, E.; Leon, O.; Torres, G.; Espidel, J. *Fuel* **2000**, *79*, 1389-1394.
5. Anastasiadis, S. H.; Gancarz, I.; Koberstein, J. T. *Macromolecules* **1988**, *21*, 2980-2987.
6. Hu, W.; Koberstein, J. T.; Lingelser, J.; Gallot, Y. *Macromolecules* **1995**, *28*, 5209-5214.
7. Mayoral, E.; Goicochea, A. G. *J. Chem. Phys.* **2013**, *138*, 094703.
8. Taber, J. *SPEJ, Soc. Pet. Eng. J.* **1969**, *9*, 3-12.
9. Wiegand, G.; Franck, E. *Ber. Bunsenges./Phys. Chem. Chem. Phys.* **1994**, *98*, 809-817.
10. Jennings, H. Y. *J. Colloid Interface Sci.* **1967**, *24*, 323-329.
11. Cai, B.; Yang, J.; Guo, T. *J. Chem. Eng. Data* **1996**, *41*, 493-496.
12. Headen, T. F.; Boek, E. S.; Skipper, N. T. *Energy Fuels* **2009**, *23*, 1220-1229.
13. Teklebrhan, R. B.; Ge, L.; Bhattacharjee, S.; Xu, Z.; Sjöblom, J. *J. Phys. Chem. B* **2012**, *116*, 5907-5918.
14. Sedghi, M.; Goual, L.; Welch, W.; Kubelka, J. *J. Phys. Chem. B* **2013**, *117*, 5765-5776.

15. Jian, C.; Tang, T.; Bhattacharjee, S. *Energy Fuels* **2013**, *27*, 2057– 2067.
16. Mikami, Y.; Liang, Y.; Matsuoka, T.; Boek, E. S. *Energy Fuels* **2013**, *27*, 1838-1845.
17. Rane, J. P.; Harbottle, D.; Pauchard, V.; Couzis, A.; Banerjee, S. *Langmuir* **2012**, *28*, 9986-9995.
18. Rane, J. P.; Pauchard, V.; Couzis, A.; Banerjee, S. *Langmuir* **2013**, *29*, 4750-4759.
19. Pauchard, V.; Rane, J. P.; Banerjee, S. *Langmuir* **2014**, *30*, 12795-12803.
20. Fan, Y.; Simon, S.; Sjöblom, *Colloids Surf., A* **2010**, *366*, 120-128.
21. Jian, C.; Poopari, M. R.; Liu, Q.; Zerpa, N.; Zeng, H.; Tang, T. *J. Phys. Chem. B* **2016** *120*, 5646– 5654.
22. Jian, C.; Poopari, M. R.; Liu, Q.; Zerpa, N.; Zeng, H.; Tang, T. *Energy Fuels* **2016**, *30*, 10228-10235.
23. Zeppieri, S.; Rodríguez, J.; López de Ramos, A. *J. Chem. Eng. Data* **2001**, *46*, 1086-1088.
24. Al-Sahhaf, T.; Elkamel, A.; Suttar Ahmed, A.; Khan, A. *Chem. Eng. Commun.* **2005**, *192*, 667-684.
25. Ikeda, N.; Aratono, M.; Motomura, K. *J. Colloid Interface Sci.* **1992**, *149*, 208-215.
26. Moeini, F.; Hemmati-Sarapardeh, A.; Ghazanfari, M.; Masihi, M.; Ayatollahi, S. *Fluid Phase Equilib.* **2014**, *375*, 191-200.

27. Speight, J. G. *The Chemistry and Technology of Petroleum*, 3rd ed.; Marcel Dekker: New York, 1999.
28. Jian, C.; Zeng, H.; Liu, Q.; Tang, T. *J. Phys. Chem. C* **2016**, *120*, 14170-14179.
29. Schuler, B.; Meyer, G.; Peña, D.; Mullins, O. C.; Gross, L. *J. Am. Chem. Soc.* **2015**, *137*, 9870-9876.
30. Yang, F.; Tchoukov, P.; Dettman, H.; Teklebrhan, R. B.; Liu, L.; Dabros, T.; Czarnecki, J.; Masliyah, J.; Xu, Z. *Energy Fuels* **2015**, *29*, 4783-4794.
31. Subramanian, S.; Simon, S.; Gao, B.; Sjöblom, J. *Colloids Surf., A* **2016**, *495*, 136-148.
32. Jian, C.; Tang, T.; Bhattacharjee, S. *Energy Fuels* **2014**, *28*, 3604– 3613.
33. Oostenbrink, C.; Villa, A.; Mark, A. E.; Van Gunsteren, W. F. *J. Comput. Chem.* **2004**, *25*, 1656-1676.
34. Berendsen, H. J. C.; Postma, J. P. M.; van Gunsteren, W.; Hermans, J. Interaction Models for Water in Relation to Protein Hydration. In *In Intermolecular Forces*; Pullmann, B., Ed., Ed.; D. Reidel Publishing Company: Dordrecht, 1981; pp 331-342.
35. Tieleman, D.; Berendsen, H. *J. Chem. Phys.* **1996**, *105*, 4871-4880.
36. Zielkiewicz, J. *J. Chem. Phys.* **2005**, *123*, 104501.
37. Kuznicki, T.; Masliyah, J. H.; Bhattacharjee, S. *Energy Fuels* **2009**, *23*, 5027-5035.

38. Hess, B.; Kutzner, C.; Van Der Spoel, D.; Lindahl, E. *J. Chem. Theory Comput.* **2008**, *4*, 435-447.
39. Van Der Spoel, D.; Lindahl, E.; Hess, B.; Groenhof, G.; Mark, A. E.; Berendsen, H. J. C. *J. Comput. Chem.* **2005**, *26*, 1701-1718.
40. Lindahl, E.; Hess, B.; van der Spoel, D. *J. Mol. Model.* **2001**, *7*, 306-317.
41. Berendsen, H. J. C.; van der Spoel, D.; van Drunen, R. *Comput. Phys. Commun.* **1995**, *91*, 43-56.
42. Essmann, U.; Perera, L.; Berkowitz, M. L.; Darden, T.; Lee, H.; Pedersen, L. G. *J. Chem. Phys.* **1995**, *103*, 8577.
43. Parrinello, M.; Rahman, A. *J. Appl. Phys.* **1981**, *52*, 7182-7190.
44. Bussi, G.; Donadio, D.; Parrinello, M. *J. Chem. Phys.* **2007**, *126*, 014101.
45. Humphrey, W.; Dalke, A.; Schulten, K. *J. Mol. Graph.* **1996**, *14*, 33-38.
46. Rosen, M. J.; Kunjappu, J. T. *Surfactants and interfacial phenomena*, 3rd ed.; Wiley-Interscience: Hoboken, NJ, 2004.
47. Harvey, R. *J. Phys. Chem.* **1958**, *62*, 322-324.
48. Ozboyaci, M.; Kokh, D. B.; Corni, S.; Wade, R. C. *Q. Rev. Biophys.* **2016**, *49*, e4.

TOC:



Tables:**Table 1.** Details of the Simulated Systems

System name	Box size (nm ³)	No. of VO-79 molecules	Temperature (K)	Pressure (bar)
T373-P100	6×6×6	0	373	100
T423-P100	6×6×6	0	423	100
T473-P100	6×6×6	0	473	100
T473-P200	6×6×6	0	473	200
T373-P100-VO180	12×12×24	180	373	100
T373-P100-VO540	12×12×24	540	373	100
T373-P100-VO720	12×12×24	720	373	100
T423-P100-VO180	12×12×24	180	423	100
T423-P100-VO540	12×12×24	540	423	100
T423-P100-VO720	12×12×24	720	423	100
T473-P100-VO180	12×12×24	180	473	100
T473-P100-VO540	12×12×24	540	473	100
T473-P100-VO720	12×12×24	720	473	100
T473-P200-VO180	12×12×24	180	473	200
T473-P200-VO540	12×12×24	540	473	200
T473-P200-VO720	12×12×24	720	473	200

Table 2. IFT values of toluene/water interface in absence of VO-79

Conditions	Simulation values (mN/m)	Experimental values (mN/m)⁹
373 K 100 bar	28.79	27.58
423 K 100 bar	23.30	23.33
473 K 100 bar	14.47	N/A
473 K 200 bar	16.59	16.66

Figures:

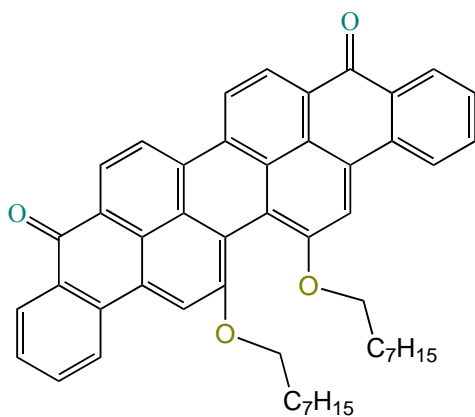


Figure 1. Chemical structure of the VO-79 compound

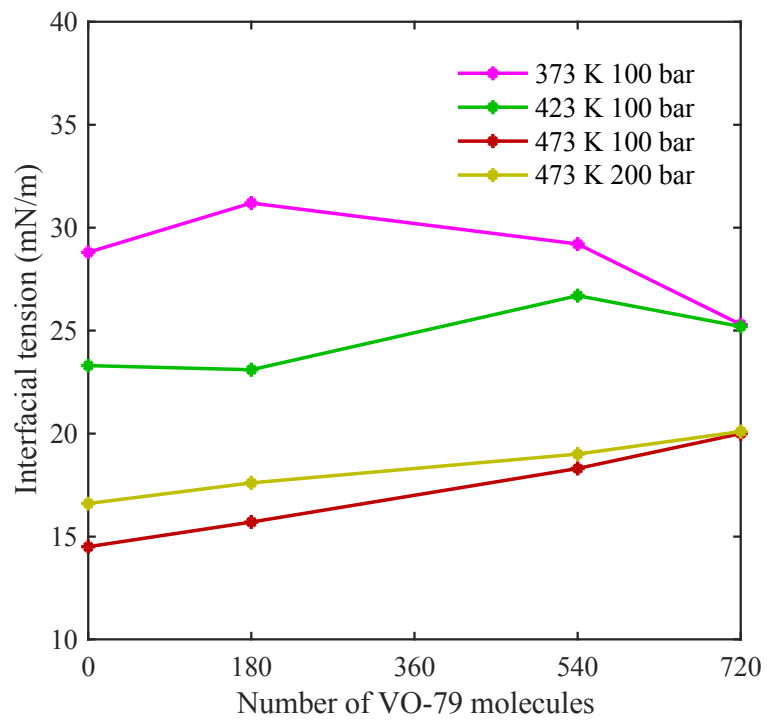


Figure 2. IFT as a function of number of VO-79 molecules.

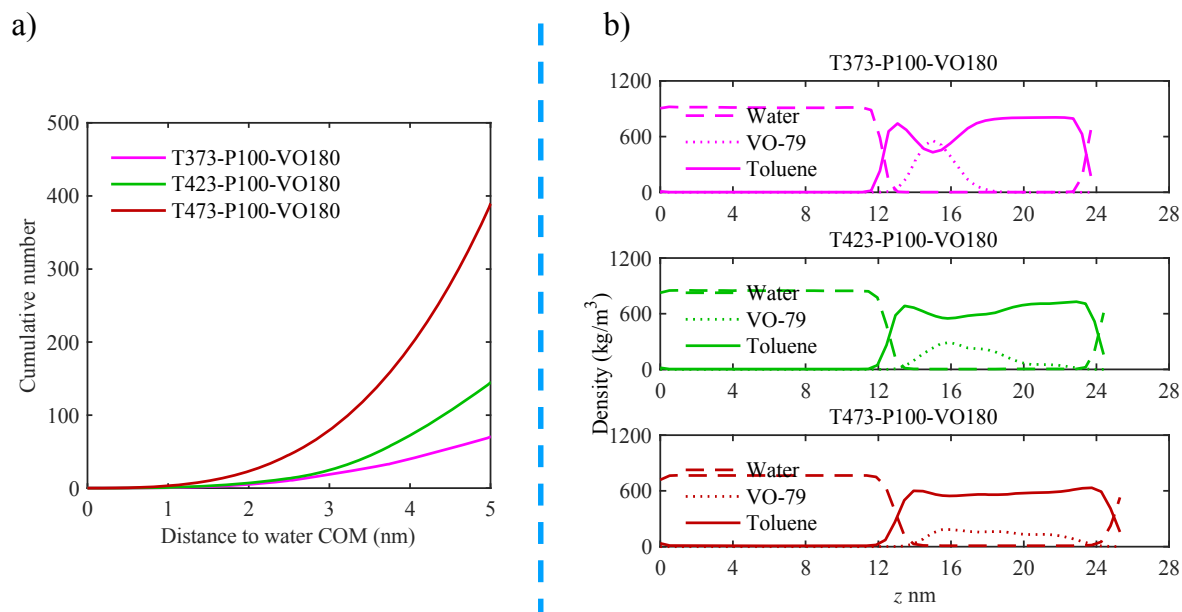


Figure 3. a) Cumulative number of toluene atoms around COM of water phase, and b) density profiles of water, toluene and VO-79 along z -axis (perpendicular to the water/toluene interface). Both plots are for the three systems containing 180 VO-79 molecules, simulated at 100 bar but at different temperatures.

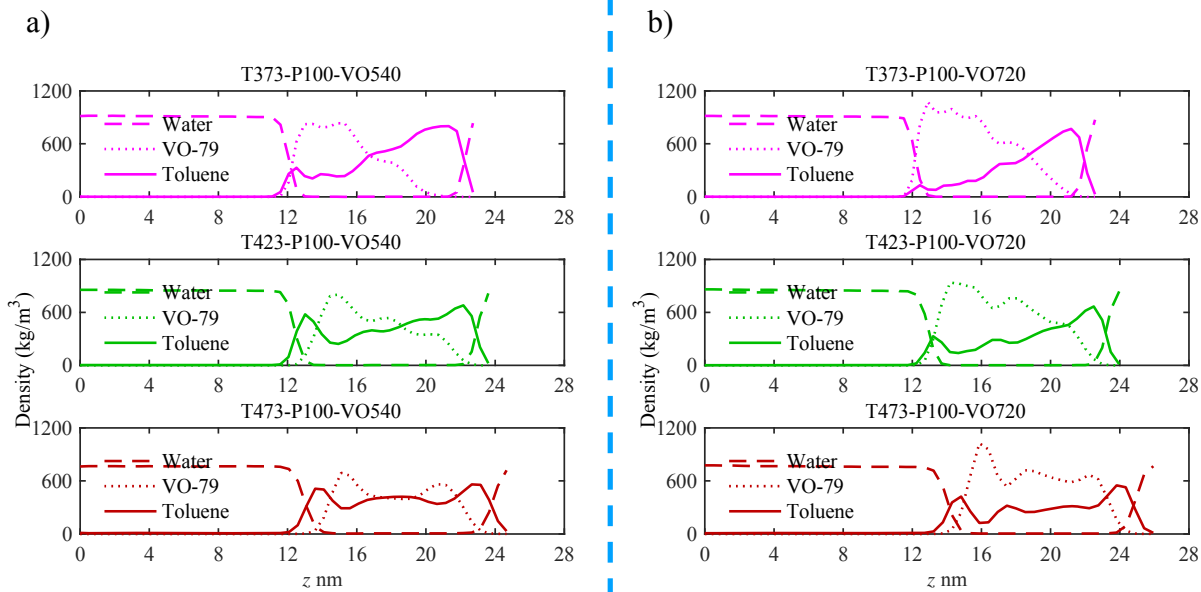


Figure 4. Density profiles in systems containing a) 540 VO-79 molecules, and b) 720 VO-79 molecules. Each subfigure consists of three plots that correspond to simulations at the same pressure (100 bar) but different temperatures.

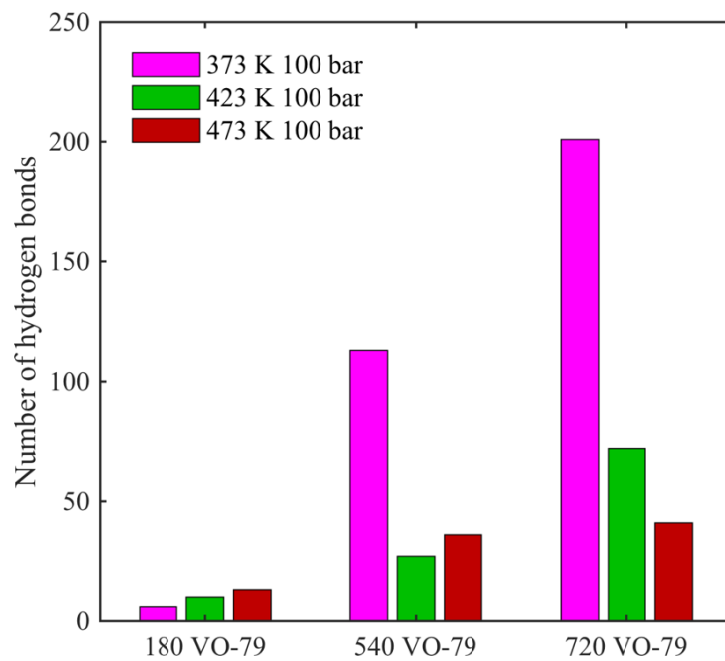


Figure 5. Number of hydrogen bonds formed between VO-79 and water molecules for systems containing different numbers of VO-79 molecules and at different T conditions.

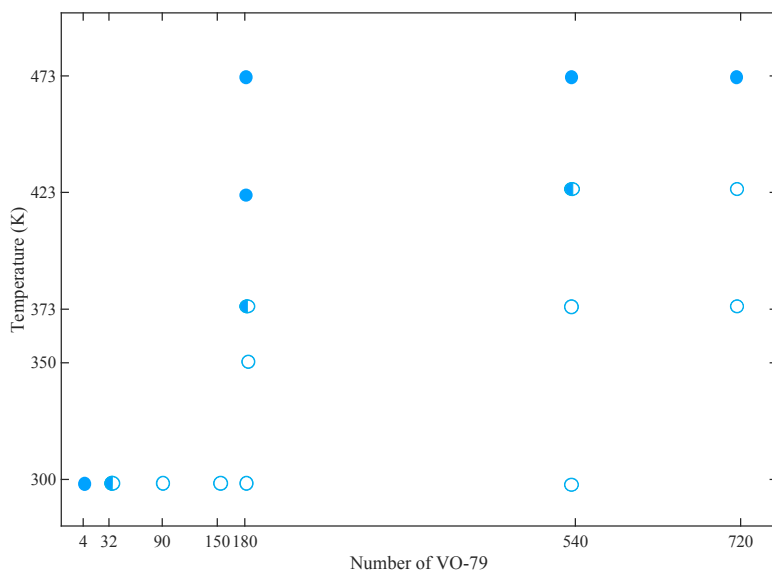


Figure 6. Roles of VO-79 at different VO-79 concentrations and different temperatures, where filled circles represent solutes, empty ones are surfactants, and half-filled ones represent transition between the two roles.